9. J. Tsuji, *Palladium Reagents and Catalysts* (Wiley, Chichester, UK, 1995).
10. A. J. Canty, *Acc. Chem. Res.* **25**, 83 (1992).
11. C. J. Elsevier, *Coord. Chem. Rev.* **185-186**, 809 (1999).
12. M.-J. Fernandez, P. M. Maitlis, *J. Chem. Soc. Chem. Commun.* **1982**, 310 (1982).
13. J. Y. Corey, J. Braddock-Wilking, *Chem. Rev.* **99**, 175 (1999).
14. M. Suginome, Y. Kato, N. Takeda, H. Oike, Y. Ito, *Organometallics* **17**, 495 (1998).
15. M. Brookhart, B. E. Grant, C. P. Lenges, M. H. Prosenc, P. S. White, *Angew. Chem. Int. Ed.* **39**, 1676 (2000).
16. S. Shimada, M. Tanaka, K. Honda, *J. Am. Chem. Soc.* **117**, 8289 (1995).
17. S. Shimada, M. Tanaka, M. Shiro, *Angew. Chem. Int. Ed. Engl.* **35**, 1856 (1996).
18. S. Shimada, M. L. N. Rao, M. Tanaka, *Organometallics* **18**, 291 (1999).
19. Ir^{V} complexes with bidentate silyl ligands were also reported [M. Loza, J. W. Faller, R. H. Crabtree, *Inorg. Chem.* **34**, 2937 (1995)].
20. W. Chen, S. Shimada, T. Hayashi, M. Tanaka, *Chem. Lett.* **2001**, 1096 (2001).
21. W. Chen, S. Shimada, M. Tanaka, unpublished data.
22. Details of synthetic procedure for complexes **1a**, **1b**, **2a**, and **2b** and NMR data for **1a** and **1b** are available at *Science* Online (*35*).
23. X-ray crystallographic analysis was carried out on a Rigaku AFC7R diffractometer using a rotating anode (58 kV, 280 mA for **2a** and 56 kV, 270 mA for **2b**) with graphite monochromated Mo-K_α radiation (λ = 0.71069 Å). Crystal data for **2a**: $C_{30}H_{52}P_4Pd_3Si_6$; MW = 1024.35; orthorhombic; space group *Fdd2*; Z = 16; T = −100° ± 1°C; a = 18.524(9) Å, b = 76.981(5) Å, c = 11.964(3) Å, and V = 17060(8) Å^3; goodness of fit = 1.05; $R1$ [$I > 2\sigma(I)$] = 0.040; $wR2$ = 0.117 (all data). Crystal data for **2b**: $C_{38}H_{68}P_4Pd_3Si_6$; MW = 1136.56; triclinic; space group *P*-1; Z = 4; T = −80° ± 1°C; a = 20.051(2) Å, b = 21.546(3) Å, c = 11.565(1) Å, α = 90.199(10)°, β = 97.188(8)°, γ = 87.893(10)°, and V = 4953.6(10) Å^3; goodness of fit = 1.89; $R1$ [$I > 2\sigma(I)$] = 0.065; $wR2$ = 0.206 (all data). Atomic coordinates, bond lengths, and angles and the other important parameters have been deposited with the Cambridge Crystallographic Data Centre as supplementary publications CCDC 174451 and 174452. Copies of the data can be obtained, free of charge, from CCDC (e-mail: deposit@ccdc.cam.ac.uk). Details of x-ray crystallographic analysis are also available at *Science* Online (*35*).
24. Y. Pan, J. T. Mague, M. J. Fink, *Organometallics* **11**, 3495 (1992).
25. M. Murakami, T. Yoshida, Y. Ito, *Organometallics* **13**, 2900 (1994).
26. M. Suginome, H. Oike, P. H. Shuff, Y. Ito, *Organometallics* **15**, 2170 (1996).
27. M. Suginome, H. Oike, S.-S. Park, Y. Ito, *Bull. Chem. Soc. Jpn.* **69**, 289 (1996).
28. Y. Tanaka, H. Yamashita, S. Shimada, M. Tanaka, *Organometallics* **16**, 3246 (1997).
29. Y.-J. Kim *et al.*, *Organometallics* **17**, 4929 (1998).
30. Y.-J. Kim *et al.*, *J. Chem. Soc. Dalton Trans.* **2000**, 417 (2000).
31. R. H. Crabtree, *Angew. Chem. Int. Ed. Engl.* **32**, 789 (1993).
32. NMR of **2a** ([D_6]benzene solution, ^{1}H) δ value (parts per million) 0.40 (doublet, 6H, $J_{P\text{-}H}$ = 7 Hz); 0.65 to 1.05 (multiplet, 8H); 0.78 (doublet, 6H, $J_{P\text{-}H}$ = 7 Hz); 0.89 (doublet, 6H, $J_{P\text{-}H}$ = 7 Hz); 1.00 (doublet, 6H, $J_{P\text{-}H}$ = 7 Hz); 4.30 (broad singlet, 2H); 5.00 to 5.20 [a sharp doublet (J = 20 Hz) and a broad multiplet are overlapped, 6H]; 8.03 to 8.08 (multiplet, 4H); 8.25 (doublet of doublet, 2H, $J_{H\text{-}H}$ = 3 and 5 Hz). Because of the low solubility of **2a**, signals for a part of aromatic hydrogens (6H) laid under the signals of the residual hydrogen signals of the solvent. ([D_6]benzene solution, ^{31}P) δ value, 21.1 (doublet, $J_{P\text{-}P}$ = 24 Hz); 21.4 (doublet, $J_{P\text{-}P}$ = 24 Hz). ^{29}Si NMR spectrum of **2a** was not obtained due to the low solubility of **2a**. NMR of **2b** ([D_8]toluene solution, ^{1}H) δ value, 0.7 to 1.7 (multiplet, 44H); 1.72 to 1.83 (multiplet, 2H); 1.93 to 2.04 (multiplet, 2H); 4.16 (broad singlet, 2H); 5.18 to 5.73 [a sharp doublet (J = 12 Hz) and a broad multiplet are overlapped, 6H]; 7.33 to 7.43 (multiplet, 6H); 8.18 (doublet, 2H, $J_{H\text{-}H}$ = 6 Hz); 8.22 (doublet, 2H, $J_{H\text{-}H}$ = 6 Hz); 8.35 (doublet of doublet, 2H, $J_{H\text{-}H}$ = 3 and 5 Hz); ([D_8]toluene solution, ^{31}P) δ value, 48.5 (doublet, $J_{P\text{-}P}$ = 24 Hz); 48.8 (doublet, $J_{P\text{-}P}$ = 24 Hz); ([D_8]toluene solution, ^{29}Si) δ value, −12.9 [doublet of doublet, $J_{P\text{-}Si}$ = 22 and 124 Hz, ($J_{H\text{-}Si}$ = 182 Hz)], *Si*H; −11.3 [singlet, ($J_{H\text{-}Si}$ = 184 Hz)], *Si*H$_2$; 20.0 [doublet of doublet of doublet, $J_{P\text{-}Si}$ = 5, 23 and 111 Hz, ($J_{H\text{-}Si}$ = 187 Hz)], *Si*H. ^{1}H-decoupled and ^{1}H-coupled ^{29}Si NMR spectra were measured. The $J_{P\text{-}Si}$ values were obtained from ^{1}H-decoupled spectrum and the number of hydrogen atoms bound to the silicon atoms and the $J_{H\text{-}Si}$ values were determined by ^{1}H-coupled spectrum. IR of **2b** (KBr pellet) 3033, 2960, 2927, 2898, 2871, 2038, 1454, 1413, 1376, 1238, 1099, 1025, 944, 865, 794, 757, 682, 626, and 449 cm^{-1}.
33. S. Shimada, M. L. N. Rao, T. Hayashi, M. Tanaka, *Angew. Chem. Int. Ed.* **40**, 213 (2001).
34. L.-B. Han, M. Tanaka, *Chem. Commun.* **1999**, 395 (1999).
35. Supplementary data are available on *Science* Online at www.sciencemag.org/cgi/content/full/295/5553/308/DC1.

36. We are grateful to the Japan Science and Technology Corporation (JST) for financial support through the CREST (Core Research for Evolutional Science and Technology) program and for a postdoctoral fellowship (to W.C.).

11 October 2001; accepted 28 November 2001

Direct Determination of the Timing of Sea Level Change During Termination II

Christina D. Gallup,[1]* H. Cheng,[2] F. W. Taylor,[3] R. L. Edwards[2]

An outcrop within the last interglacial terrace on Barbados contains corals that grew during the penultimate deglaciation, or Termination II. We used combined ^{230}Th and ^{231}Pa dating to determine that they grew 135.8 ± 0.8 thousand years ago, indicating that sea level was 18 ± 3 meters below present sea level at the time. This suggests that sea level had risen to within 20% of its peak last-interglacial value by 136 thousand years ago, in conflict with Milankovitch theory predictions. Orbital forcing may have played a role in the deglaciation, as may have isostatic adjustments due to large ice sheets. Other corals in the same outcrop grew during oxygen isotope (δ^{18}O) substage 6e, indicating that sea level was 38 ± 5 meters below present sea level, about 168.0 thousand years ago. When compared to the δ^{18}O signal in the benthic V19-30/V19-28 record at that time, the coral data extend to the previous glacial cycle the conclusion that deep-water temperatures were colder during glacial periods.

The timing of the penultimate deglaciation (Termination II) has fundamental implications for the causes of climate change. Terminations, as distinct climatic events, provide an opportunity to test the Milankovitch theory of orbital forcing of the glacial cycles, which holds that increases in summer insolation at high Northern latitudes should precede or coincide with glacial melting and, similarly, that decreases should precede or coincide with glacial growth. However, despite decades of studies aimed at constraining the timing of sea level change during Termination II, the question of whether its timing is consistent with Milankovitch theory predictions remains unanswered. As direct indicators of sea level, corals are a potential resource for addressing the problem. The main hurdles have been: (i) finding corals that record sea level during Termination II and (ii) demonstrating that uranium-series ages have remained unchanged by the effects of diagenesis. We have identified Termination II corals on Barbados and have tested them for diagenesis using combined ^{230}Th and ^{231}Pa dating.

Two efforts to date Termination II, from Devils Hole, in Nevada, United States (*1*) and Bahamian coastal sediments (*2*), suggest that the deglaciation occurred too early to have been caused directly by orbital forcing. ^{230}Th dating of the Devils Hole calcite vein isotopic oxygen (δ^{18}O) record (*3*, *4*) places the midpoint of the δ^{18}O rise during Termination II at 140 ± 3 thousand years ago (ka), 6 ± 3 thousand years before the midpoint in the rise of 65°N summer insolation. U-Th isochron dating of carbonate sediments from the slopes of the Bahamas places the midpoint of the marine δ^{18}O rise at 135 ± 2.5 ka (*2*), within error of the midpoint of the rise in 65°N summer insolation. Although these data are compelling, questions remain (*5*) because neither record is a direct measure of sea level.

[1]Department of Geological Sciences, University of Minnesota Duluth, Duluth, MN 55812, USA. [2]Minnesota Isotope Laboratory, Department of Geology and Geophysics, University of Minnesota, Minneapolis, MN 55455, USA. [3]Institute for Geophysics, University of Texas at Austin, Austin, TX 78712, USA.

*To whom correspondence should be addressed. E-mail: cgallup@d.umn.edu

Our study focuses on a particular site in Barbados that has optimal features for looking for Termination II corals. The site is in the last interglacial terrace (also known as the First High Cliff or the Rendezvous Hill terrace) on the southwest side of the island [transect B in (*6*)]. It also has the highest uplift rate on the island (0.44 m per thousand years), associated with the creation of the Clermont-Nose anticline (*7*). Thus, it has the best potential for containing samples that grew during Termination II. A new excavation along the roadcut below the University of the West Indies campus allowed careful examination of the deposits within the last interglacial terrace (Fig. 1). We collected samples from several distinct units (Fig. 1) occurring below and partially buried by the forereef deposits of the last interglacial reef, because these units would be most likely to include Termination II material. We also collected samples from two units that showed promise of including corals that grew just before and after the last interglacial. Samples were collected in the vicinity of sample UWI-2 (*6*), which has generated interest (*8*) because of its last interglacial age (129.1 ± 0.8 ka) and low initial sea level (–25 ± 5 m). Site OC (*9*), on the slope below the campus and 180 m west of the roadcut transect (Fig. 1), was targeted for corals that grew after the last interglacial because it does not appear buried by last interglacial forereef deposits.

We applied high-precision ^{230}Th and ^{231}Pa dating methods (*10*–*12*) to multiple samples from each of these units (Table 1); complete results are available as Web table 1 (*13*). ^{231}Pa dating was applied in addition to ^{230}Th dating to improve our ability to identify samples with accurate ages that could be used to build a sea level record. Although no test guarantees accuracy, ^{231}Pa dating is an important check for the effects of diagenetic processes that can shift ^{230}Th ages and is the only other chronometer in this time range (500 ka) that has a precision close to that of ^{230}Th (*12*). The parents and daughters of both chronometers are similar chemically: Th and Pa have similar chemical affinities and both have a uranium parent isotope.

We previously developed a method for screening out altered samples based on an observed correlation between initial δ^{234}U values and ^{230}Th ages, so that samples with initial δ^{234}U values within 8 per mil (‰) of the modern value should have ^{230}Th ages accurate to within 2000 years of the true age (*6*, *14*). However, data from (*12*) and this study include samples that fall within the 8‰ δ^{234}U envelope but have discordant ^{231}Pa and ^{230}Th ages [Web fig. 1 (*13*)]. This suggests that the δ^{234}U criterion is not sufficient to identify all samples that have experienced diagenetic alteration and that ^{231}Pa dating is necessary to screen out such samples.

On the basis of this analysis, the concordancy of ^{230}Th and ^{231}Pa dates is our best test that the ages have not been shifted by diagenetic alteration. Samples OC-1, OC-2, UWI-101, NU-1471, NU-1472, NU-1473, and NU-1464 in Table 1 have concordant ^{231}Pa and ^{230}Th ages (*15*). Two additional criteria that help to confirm the absence of diagenetic effects (*16*) include (i) no evidence of recrystallization of aragonite to calcite and (ii) an initial δ^{234}U value within 8‰ of the modern value. Samples that meet all three criteria are most likely to record accurate ages; those that meet fewer than three are less likely to have accurate ages, although they still may hold valuable climatic information. Further, samples (Table 1) must be considered in the context of existing data [Web table 1 (*13*) and previous high-precision U-series data from this locality (*6*, *12*)] for us to be able to evaluate stratigraphic consistency and to interpret the stratigraphy.

For Termination II, precision and accuracy in chronometry are critical. Samples NU-1471, NU-1472, and NU-1473 are from units below the last interglacial reef deposits (Fig. 1), and all have concordant ^{231}Pa and ^{230}Th ages. Their ages, clustering around 135 ka, and initial elevations, 16 to 18 m below present sea level (Table 1), suggest that they formed during the rise to peak interglacial sea level (Termination II). Samples NU-1471 and NU-1472 are from the mixed *Acropora palmata* and head coral unit, just below the cobble-rich unit of sample NU-1473. All give similar ages, demonstrating stratigraphic consistency and a genetic relationship between the two units. The presence of the cobbles suggests a proximity to sea level during the time recorded by these samples. Sample NU-1471 not only has concordant ^{231}Pa and ^{230}Th ages but meets the other two criteria as well, indicating that the timing of this sea level event during Termination II was 135.8 ± 0.8 ka (*17*).

Sample UWI-101, collected adjacent to sample UWI-2 (*6*), also meets all three criteria and confirms the age of the deposit as 129.1 ± 0.5 ka. Surprisingly, samples immediately adjacent to these samples (Fig. 1) give ages that correspond to marine oxygen-isotope event 6.5 (*18*). The UWI-101 unit is distinct from the surrounding stage 6 material (*19*); however, the unit is not sufficiently exposed to determine whether it is in place. Thus, the initial sea level of 25 ± 3 m below present sea level implied by UWI-101 and UWI-2 remains tentative.

Sample OC-1 also meets all three criteria, giving an age of 113.6 ± 0.4 ka. The beach-like nature of the upper OC deposit (*9*) sug-

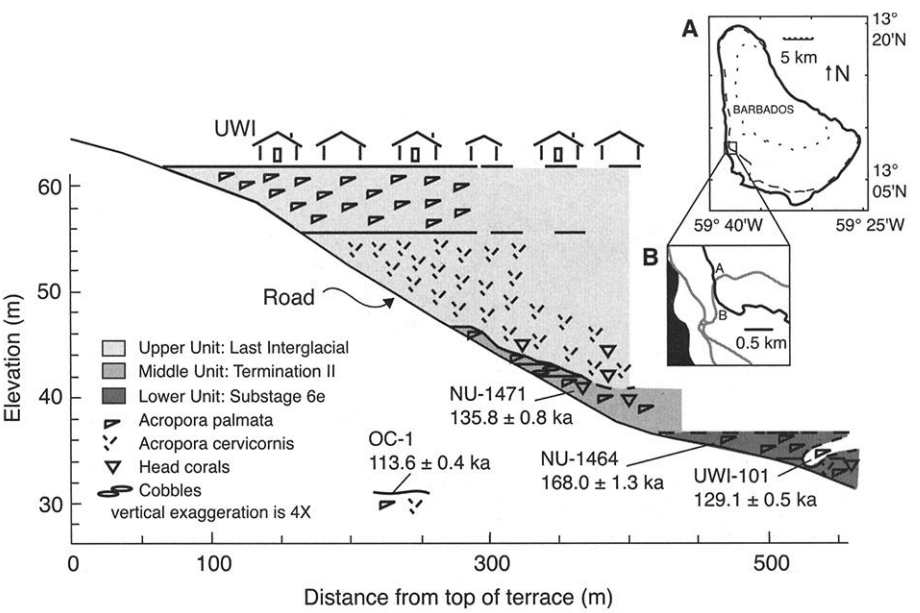

Fig. 1. Transect of last interglacial terrace below the University of the West Indies (UWI), showing approximate sample locations (the OC-1 and OC-2 deposit is projected onto the transect for reference). The upper unit includes the reefcrest and forereef deposits of the last interglacial reef. The forereef deposit overlies and partially buries a series of deposits, divided into a middle unit and a lower unit. The middle unit is composed of a series of three distinct deposits: an *A. palmata*–rich deposit overlying a coral cobble deposit, which in turn overlies a deposit with mixed *A. palmata* and head corals. The lower unit has an *A. palmata*–rich deposit overlying a mixed *A. palmata*, *A. cervicornis*, and head coral zone. The relationship between the middle and lower unit is obscured by vegetation. (**A**) Map of Barbados showing the region of sample collection, the First High Cliff (last interglacial terrace; dashed line), and the Second High Cliff (dotted line). (**B**) Map of region showing location of the sampling transect (A and B represent top-left and lower-right locations, respectively on transect), the crest of the last interglacial terrace (thin black line), and roads (thick gray lines).

gests that it represents a fall to 19 m below present sea level from peak last-interglacial sea level (+6 m). However, sample OC-2 also has concordant ^{230}Th and ^{231}Pa ages, and although its δ^{234}U value is somewhat elevated, its ^{230}Th age of 105.3 ± 0.6 ka puts it squarely in substage 5c. Thus, it is also possible that the deposit is from substage 5c [in agreement with (*20*)], giving an initial sea level of 15 ± 3 m below present sea level and that sample OC-1 was reworked from material deposited during the fall from peak last-interglacial sea level.

Sample NU-1464 has concordant ^{230}Th and ^{231}Pa ages, a marine initial δ^{234}U value, and a ^{230}Th age of 168.0 ± 1.3 ka, suggesting a correlation with marine oxygen isotope event 6.5. Although it was found to have a small amount of detectable calcite, its age is supported by other samples from the unit with similar ages and initial δ^{234}U values (Table 1). Using sample NU-1464 as the best-preserved sample, we calculate an initial sea level of 8 ± 5 m below present sea level.

Figure 2B summarizes the sea level record suggested by the new data. Most significantly, our record includes corals that document sea level directly during Termination II, suggesting that the majority (~80%) of the Termination II sea level rise occurred before 135 ka. This is broadly consistent with early shifts in δ^{18}O recorded in the Bahamas (*2*) and Devils Hole (*1*) (Fig. 2C) and with early dates (134 ka) of last interglacial corals from Hawaii (*21*), which call into question the timing of Termination II in the SPECMAP record (*22*) (Fig. 2C). Our record also echoes some of the coral results from Papua New Guinea, which suggested a sea level rise peaking ~135 ka (*23*), followed by a sea level drop ~129 ka (*24*), followed in turn by a rapid rise to peak last-interglacial sea level. However, it does not confirm the drop to –90 m at 129 ka suggested in the Aladdin's Cave study (*24*).

The discovery of corals that grew during substage 6e is the first well-documented measure of sea level from this period. Assuming that sample NU-1464 represents peak sea level, there may be correlative peaks in the benthic record of V19-30/V19-28 (*25*) and Vostok atmospheric δ^{18}O (*26*) (Fig. 2D) records, but the amplitudes are quite different. Normalizing the coral and V19-30/V19-28 records to their glacial-interglacial ranges, the coral sea level at substage 6e is ~34% (44 out of 130 m) below the maximum sea level (+6 m), and the V19-30/V19-28 δ^{18}O peak is ~60% heavier than the substage 5e peak. This difference implies a significant temperature component to the benthic δ^{18}O curve, due to colder temperatures in the deep sea, as has been suggested for the last glacial cycle (*27*, *28*). The substage 6e data generalize the phenomenon to the previous glacial cycle. The Vostok atmospheric δ^{18}O record, conversely, is only 13% heavier than the peak substage 5e value. Shackleton (*25*) used this record to convert the benthic δ^{18}O record to sea level change and came up with a sea level close to interglacial levels at this time. The coral record agrees most closely with the Lea *et al.* (*29*) resid-

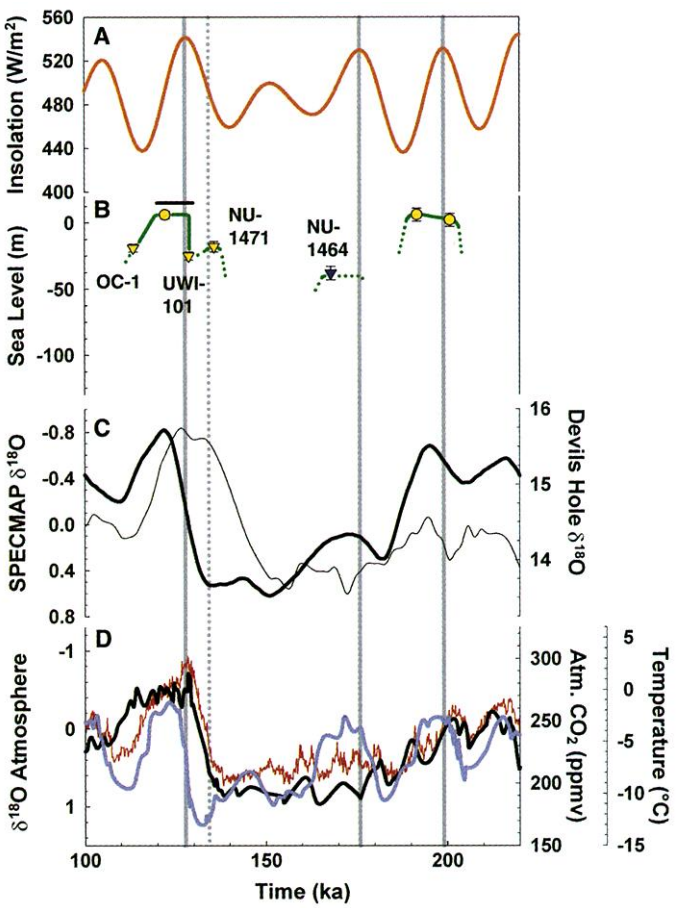

Fig. 2. (**A**) 65°N June insolation (*38*). The solid gray vertical lines provide a reference for peaks in insolation, and the dotted gray vertical line provides a reference for the half-peak height of the insolation rise between 140 and 130 ka. (**B**) Sea level record reconstructed from Barbados corals with concordant ^{230}Th and ^{231}Pa ages from this study (triangles, as labeled) and from (*12*) (circles); samples that meet all three criteria (see text) are in yellow; the sample in blue meets two criteria. (**C**) SPECMAP benthic δ^{18}O stack (*22*) (thick line) and Devils Hole δ^{18}O record (thin line) (*1*). (**D**) Vostok records (*26*) of atmospheric δ^{18}O (blue), atmospheric CO_2 concentration (black), and temperature from deuterium measurements (red).

Table 1. Uranium-series and other relevant information for samples [Web table 1 (*13*)] referred to in the text. Uranium-series isotopic compositions are weighted averages, where applicable [Web table 1 (*13*)]. Errors are 2σ.

Sample number	Elevation (m)	Coral species*	Calcite (weight %)†	δ^{234}U measured‡	^{230}Th/^{238}U activity§	^{231}Pa/^{235}U activity§	^{231}Pa age (ka)§	^{230}Th age (ka)§	δ^{234}U initial‖	Initial elevation (m)¶
OC-1	31	Ap	–	108.5 ± 0.7	0.7274 ± 0.0012	0.9020 ± 0.0056	109.8 + 2.8/–2.6	113.6 ± 0.4	142.6 ± 1.2	–19 ± 3
OC-2	31	Ap	4	117.1 ± 1.2	0.7013 ± 0.0021	0.8889 ± 0.0060	103.9 + 2.6/–2.5	105.3 ± 0.4	157.7 ± 1.6	–15 ± 3
UWI-101	32	Ap	–	104.5 ± 0.7	0.7776 ± 0.0013	0.9318 ± 0.0035	126.9 +2.6/–2.4	129.1 ± 0.5	150.3 ± 1.0	–25 ± 3
NU-1471	42	S	–	102.4 ± 1.1	0.7970 ± 0.0024	0.9440 ± 0.0051	136.2 ± 4.3	135.8 ± 0.8	150.3 ± 1.7	–18 ± 4
NU-1472	42	Ap	1	111.5 ± 1.0	0.8056 ± 0.0024	0.9419 ± 0.0062	134.5 ± 5.0	136.1 ± 0.8	163.7 ± 1.6	–18 ± 4
NU-1473	43	Ap	–	107.3 ± 1.0	0.7963 ± 0.0024	0.9404 ± 0.0055	133.3 ± 4.4	134.2 ± 0.8	156.7 ± 1.5	–16 ± 4
NU-1464	36	Ap	2	95.7 ± 1.2	0.8760 ± 0.0028	0.9664 ± 0.0061	160.4 ± 8.5	168.0 ± 1.3	153.8 ± 2.1	–38 ± 5
UWI-103	34	Ap	–	96.6 ± 1.2	0.8928 ± 0.0027	0.9671 ± 0.0131	161 + 24/–16	175.3 ± 1.4	158.5 ± 2.0	–43 ± 5
UWI-107	32	Ap	–	91.2 ± 1.2	0.8768 ± 0.0027	0.9593 ± 0.0069	151.3 + 8.8/–7.4	170.3 ± 1.3	147.6 ± 2.0	–43 ± 5

*Ap = *A. palmata*; S = *Siderastria*. †Measurements were made by x-ray diffraction at the University of Maryland College Park. ‡$\delta^{234}U = [(^{234}U/^{238}U)_{activity} - 1] \times 1000$. §Activities and ages were calculated using $\lambda_{230} = 9.1577 \times 10^{-6}$ year^{-1}, $\lambda_{234} = 2.8263 \times 10^{-6}$ year^{-1}, $\lambda_{238} = 1.55125 \times 10^{-10}$ year^{-1}, $\lambda_{231} = 2.1158 \times 10^{-5}$ year^{-1}, and $\lambda_{235} = 9.8485 \times 10^{-10}$ year^{-1} [age equations and references for λs are from (*39*)]. ‖$\delta^{234}U_{initial}$ was calculated based on ^{230}Th age (*T*); i.e., $\delta^{234}U_{initial} = \delta^{234}U_{measured} \times e^{\lambda 234 \times T}$. ¶Initial elevation = present elevation – (^{230}Th age × uplift rate); uplift rate is 0.44 m per thousand years; errors were reduced quadratically.

ual $\delta^{18}O$ record, which has substage 6e ~22% below peak last-interglacial values.

The Milankovitch theory in its simplest form cannot explain Termination II, as it does Termination I (*30*). However, it is still plausible that insolation forcing played a role in the timing of Termination II. As deglaciations must begin while Earth is in a glacial state, it is useful to look at factors that could trigger deglaciation during a glacial maximum. These include (i) sea ice cutting off a moisture source for the ice sheets (*31*); (ii) isostatic depression of continental crust (*32*); and (iii) high Southern Hemisphere summer insolation (*2*) through effects on the atmospheric CO_2 concentration (*33*, *34*). If ice sheets remained large during much of stage 6, the isostatic depression of the crust could have lowered the elevation of the ice sheets enough for a significant proportion of the ice sheets to have been below the equilibrium line by 145 ka, causing collapse and melting. Combined with the moisture-starving effects of extensive sea ice and the warming effects of rising CO_2 concentrations, isostatic effects could explain the early deglaciation. Further, Johnson (*35*) found a minimum in the gradient between high- and low-latitude insolation in the Northern Hemisphere at 140 ka, which would also decrease the moisture source for the ice sheets. Such a scenario would agree with models suggesting that isostatic adjustments associated with large ice sheets are a significant factor in creating the 100,000-year cycle (*32*), which is largely defined by glacial terminations.

Because there is no single clear driving mechanism for an early sea level rise during Termination II, it poses a challenge to the Milankovitch theory. The timing and cause of Termination II are particularly important because it is so closely linked to the 100,000-year cycle, of which the driving mechanism remains unclear and widely debated (*36*). With the timing of only two glacial terminations known precisely enough to test Milankovitch theory predictions, it is difficult to identify which termination is the anomaly. Corals and speleothem data from earlier terminations may help resolve the problem.

References and Notes

1. I. Winograd *et al.*, *Science* **258**, 255 (1992).
2. G. Henderson, N. Slowey, *Nature* **404**, 61 (2000).
3. K. R. Ludwig *et al.*, *Science* **258**, 284 (1992).
4. I. J. Winograd, J. M. Landwehr, K. R. Ludwig, T. B. Coplen, A. C. Riggs, *Quat. Res.* **48**, 141 (1997).
5. T. D. Herbert *et al.*, *Science* **293**, 71 (2001).
6. C. D. Gallup, R. L. Edwards, R. G. Johnson, *Science* **263**, 796 (1994).
7. F. W. Taylor, P. Mann, *Geology* **19**, 103 (1991).
8. M. T. McCulloch, T. Esat, *Chem. Geol.* **169**, 107 (2000).
9. The OC site has two outcrops, both in roadcuts on a small road off of the main coastal highway and perpendicular to the shore. One outcrop is at the intersection with the coastal highway at an ~20-m elevation, and the other is one block uphill in a low-lying terrace at an ~30-m elevation. The lower outcrop (samples OC-4 and OC-5) contains *A. palmata* and *A. cervicornis* coral fragments, and the upper outcrop (samples OC-1 and OC-2) contains coral fragments of the same species in a loose, well-sorted carbonate sand with abundant shells and is likely part of a beach deposit. The lower outcrop is at the same elevation and approximate location as the OC site in Mesollela *et al.* (*20*) and Bender *et al.* (*37*); the upper is at the same elevation and adjacent to site AFK in (*20*) and (*37*).
10. R. L. Edwards, J. H. Chen, G. J. Wasserburg, *Earth Planet. Sci. Lett.* **81**, 175 (1987).
11. R. L. Edwards, J. H. Chen, T. L. Ku, G. J. Wasserburg, *Science* **236**, 1547 (1987).
12. R. L. Edwards, H. Cheng, M. T. Murrell, S. J. Goldstein, *Science* **276**, 782 (1997).
13. Supplementary Web material is available on *Science* Online at www.sciencemag.org/cgi/content/full/295/5553/310/DC1.
14. There could be significant error associated with the empirical model used to produce the 2000-year constraint on the accuracy of ^{230}Th ages for samples with initial $\delta^{234}U$ values within 8‰ of the modern value. Thus, it is only meant to be a rough guide to sample preservation, not a tool for correcting ages.
15. As errors vary for ^{231}Pa dates, concordancy is defined as matching within 3% of the ^{231}Pa age for samples with errors of 3% or less.
16. Other important criteria for well-preserved samples, which all of our samples meet, include (i) no evidence of inherited ^{230}Th, as indicated by a low ^{232}Th concentration; and (ii) a U concentration similar to that of modern corals of the same species.
17. The error quoted for NU-1471 and the other samples represents the 2σ analytical error. There is also systematic error associated with the error in the half-lives, which contributes ±400 years for a sample of ~130 ka. Possible errors associated with diagenetic alteration are not included and are difficult to quantify.
18. D. G. Martinson *et al.*, *Quat. Res.* **27**, 1 (1987).
19. The UWI-101 (Fig. 1) deposit is distinct from the downslope stage 6 material because UWI-101 does not contain head corals; its contact with the upslope stage 6 material is marked by an erosional surface that truncates a head coral (sample UWI-107).
20. K. J. Mesolella, R. K. Matthews, W. S. Broecker, D. L. Thurber, *J. Geol.* **77**, 250 (1969).
21. D. R. Muhs, K. R. Simmons, B. Steinke, *Quat. Sci. Rev.*
22. J. Imbrie *et al.*, in *Milankovitch and Climate*, A. L. Berger *et al.*, Eds. (Reidel, Hingham, MA, 1984), vol. 1, pp. 269–305.
23. M. Stein *et al.*, *Geochim. Cosmochim. Acta* **57**, 2541 (1993).
24. T. M. Esat, M. T. McCulloch, J. Chappell, B. Pillans, A. Omura, *Science* **283**, 197 (1999).
25. N. J. Shackleton, *Science* **289**, 1897 (2000).
26. J. R. Petit *et al.*, *Nature* **399**, 429 (1999).
27. J. Chappell, N. J. Shackleton, *Nature* **324**, 137 (1986).
28. J. Chappell *et al.*, *Earth Planet. Sci. Lett.* **141**, 227 (1996).
29. D. W. Lea, D. K. Pak, H. J. Spero, *Science* **289**, 1719 (2000).
30. R. G. Fairbanks, *Nature* **342**, 637 (1989).
31. H. Gildor, E. Tziperman, *Paleoceanography* **15**, 605 (2000).
32. W. R. Peltier, W. T. Hyde, *J. Atmos. Sci.* **44**, 1351 (1986).
33. J. Imbrie *et al.*, *Paleoceanography* **7**, 701 (1992).
34. W. S. Broecker, G. M. Henderson, *Paleoceanography* **13**, 352 (1998).
35. R. G. Johnson, *Geology* **19**, 686 (1991).
36. D. B. Karner, R. A. Muller, *Science* **288**, 2143 (2000).
37. M. L. Bender *et al.*, *Geol. Soc. Am. Bull.* **90**, 577 (1979).
38. A. L. Berger, *Quat. Res.* **9**, 139 (1978).
39. H. Cheng *et al.*, *Chem. Geol.* **169**, 17 (2000).

40. C.D.G. thanks the Geology Department at the University of Maryland College Park for their support, including access to their x-ray diffraction equipment. We all thank the reviewers for helpful comments; R. Speed for key samples; R. G. Johnson and R. E. Higashi for help in the field; and L. H. Barker, chief Geologist of Barbados, and other Barbadians for assistance. Supported by NSF grants EAR-9712037, ESH-9809459, and OCE-9810724 and National Geographic grant 4887-92.

17 August 2001; accepted 21 November 2001

Iron-Silicon Alloy in Earth's Core?

Jung-Fu Lin,[1]* Dion L. Heinz,[1,2] Andrew J. Campbell,[1] James M. Devine,[1] Guoyin Shen[3]

We have investigated the phase relations in the iron-rich portion of the iron-silicon (Fe-Si) alloys at high pressures and temperatures. Our study indicates that Si alloyed with Fe can stabilize the body-centered cubic (bcc) phase up to at least 84 gigapascals (compared to ~10 gigapascals for pure Fe) and 2400 kelvin. Earth's inner core may be composed of hexagonal close-packed (hcp) Fe with up to 4 weight percent Si, but it is also conceivable that the inner core could be a mixture of a Si-rich bcc phase and a Si-poor hcp phase.

Iron is the most abundant element in Earth's core. However, the density of the outer core is about 10% lower than the density of Fe at the pressure and temperature conditions of the outer core, indicating the presence of a low atomic weight component (such as H, C, O, Si, or S) in the core (*1*). There is also evidence that the inner core may be less dense than pure Fe, and the proportion of light elements in the inner core may be as much as 3 weight % (*2–4*). The cosmochemical abundance of silicon and measured thermoelastic properties of non-silicon alloys indicate that silicon may be an important alloying element in the outer core (*5*, *6*), but it was excluded as the primary alloying element in the outer core on the basis of the equation of state (EOS) of the intermediate compound

[1]Department of the Geophysical Sciences, [2]James Franck Institute, [3]Consortium for Advanced Radiation Sources, University of Chicago, Chicago, IL 60637, USA.

*To whom correspondence should be addressed. E-mail: afu@geosci.uchicago.edu